Article ID: 1003 - 6326(2005)01 - 0108 - 05

Microstructure characterization of reinforcements in in-situ synthesized composites of Al-Zr-O system ①

ZHAO Yu-tao(赵玉涛), DAI Qi-xun(戴起勋), CHENG Xiao-nong(程晓农), LIN Dong-yang(林东洋), CAI Lan(蔡 兰)

(School of Materials Science and Engineering, Jiangsu University, Zhenjiang 212013, China)

Abstract: A novel in-situ reaction system Al-Zr-O was developed. In-situ Al_3Zr and Al_2O_3 particulates reinforced aluminum matrix composites were fabricated by the direct melt reaction technique in the Al-Zr-O system. Microstructures of the composites and crystal morphology of in-situ formed Al_3Zr and Al_2O_3 particulates were analyzed by scanning electron microscope (SEM) and transmission electron microscope (TEM). Results indicate that in-situ formed Al_3Zr and Al_2O_3 particles are finer and well distributed in aluminum matrix. Al_3Zr particulates with a tetragonal structure are mainly in the shape of polyhedron. A few of them are in the form of rectangle. The length/width ratio of the rectangular Al_3Zr is less than 2.0 and the maximum size is 2 μm. In addition, a certain number of Al_2O_3 submicro particles with a hexagonal structure are also generated in this system. Furthermore, it is found that Al_3Zr crystal grows by the mechanism of twinning. The twin plane is $(1\bar{1}\bar{4})$. The twinning direction is $[2\bar{2}1]$. The tensile tests show that the composites synthesized in the Al-Zr-O system exhibits high strength and ductility. There are a lot of ripples with fine particles on the fracture. The principal strengthening mechanisms for $(Al_3Zr+Al_2O_3)_p/Al$ composites may include Orowan strengthening, grain-refining strengthening, solid-solution strengthening and dislocation strengthening.

Key words: in-situ synthesis; composites; Al-Zr-O; reinforcements

CLC number: TB331; TG146.2 **Document code:** A

1 INTRODUCTION

The attractive physical and mechanical properties of aluminum matrix composites (AMCs), such as high specific modulus, strength, and thermal stability have been documented extensively[1-4]. In recent years, much attention has been paid to the development of an effective fabrication process for aluminum matrix composite. In the in-situ fabrication process, the spontaneous reaction between the reactants is utilized to synthesize reinforcements in the aluminum matrix. Thus it is expected that the in situ formed composites may reveal not only excellent dispersion of fine reinforcing particles, but also high strength and thermodynamic stability. Some of in-situ techniques include XD™, DIMOX™, PRIMEX™, VLS, LSM, and SHS[5, 6]. Especially, the direct melt reaction technique (DMR) is of simplicity, low cost and possibility of near net-shape forming and considered to be one of the most promising in-situ synthesis techniques of commercial production[7]. Up to now, however, in-situ reaction systems are mainly concentrated on Al-Ti-X, for example, Al-Ti-O, Al-Ti-B and Al-Ti-C. In-situ formed reinforcements are only focused on a few particles such as Al_3Ti, Al_2O_3, TiB_2, TiC[8].

The present work developed a novel in-situ reactive system Al-Zr-O, in which novel $(Al_3Zr+Al_2O_3)_p/Al$ composites were fabricated by the direct melt reaction between zirconium oxychloride with molten aluminum. The dispersion behavior of particles formed by the in situ reaction process, the crystal morphology and growth mechanism of in situ formation of reinforcements in aluminum matrix were investigated, and the mechanical properties and strengthening mechanism of in-situ composites were discussed.

2 EXPERIMENTAL

The raw materials were pure industrial aluminum ingot (99.85%) and zirconium oxychloride ($ZrOCl_2 \cdot 8H_2O$) powder (99.92%). Zirconium oxychloride was pre-heated at 250 ℃ for 3 h to dehydrate the bounded water in it. At the same time, 3 kg aluminum ingot was melted in RL100-60H graphite crucible in an electric furnace, and held at

① **Foundation item:** Project(50471050) supported by the National Natural Science Foundation of China; Project(00170) supported by the Key Foundation of the Ministry of Education of China; Project(BE2002039) supported by Jiangsu Provincial Key Project of Science and Technology; Project(JH02-039) supported by Jiangsu Provincial Development Project of High and New Technology of China

Received date: 2004 - 08 - 10; **Accepted date:** 2004 - 10 - 28

Correspondence: ZHAO Yu-tao, Professor; Tel: + 86--; E-mail: Zhaoyt@ujs.edu.cn

800 ℃. Then 380 g dehydrated $ZrOCl_2$ powder was added to the molten aluminum and pushed down into the melt. Subsequently liquid aluminum reacted with $ZrOCl_2$ to produce Al_3Zr and Al_2O_3. Finally, the composite melt was cast into permanent mould at 720 ℃ and the $(Al_3Zr+Al_2O_3)_p/Al$ composites were fabricated.

The as-cast composite ingots were sectioned into samples for SEM, XRD and TEM. The thin slices (d10 mm × 0.5 mm) for transmission electron microscope (TEM) were mechanically ground on 1000 grit silicon carbide paper, polished to approximately 60 μm in thickness, and subsequently thinned using argon-ion beam at 5 kV, 4mA at angles 30° and 10°. The foils prepared were carefully examined using JEM-2000EX transmission electron microscope equipped with a double-tilt holder and operated at 120 kV.

3 RESULTS AND DISCUSSION

3.1 X-ray diffraction and microstructure

Fig. 1(a) shows the X-ray diffraction pattern of the composite synthesized by the direct melt reaction between zirconium oxychloride and molten aluminum. It is illustrated that the reinforced phases in the Al-Zr-O system are Al_3Zr and α-Al_2O_3. The metallurgical reactions in the molten aluminum are as follows:

$$2ZrOCl_2 = ZrCl_4(g) + ZrO_2(s) \quad (1)$$

$$3ZrCl_4(g) + 4Al(l) = 3[Zr] + 4AlCl_3(g) \quad (2)$$

$$3ZrO_2 + 4Al(l) = 3[Zr] + 2Al_2O_3 \quad (3)$$

$$[Zr] + 3Al(l) = Al_3Zr \quad (4)$$

Fig. 1(b) shows the SEM microstructure of $(Al_3Zr+Al_2O_3)_p/Al$ composites. It is indicated that the in-situ synthesized Al_3Zr and Al_2O_3 particles are well distributed in the aluminum matrix. The maximum size of those particles is 2 μm. The morphology of them is mainly polyhedron.

3.2 Crystal morphology and growth

Fig. 2 shows the crystal morphology, TEM diffraction pattern and growth model of Al_3Zr reinforcement. There are two shapes of Al_3Zr crystal. One is polyhedral (Fig. 2(a)), the other is rectangular (Fig. 2(b)). The length/width ratio of the rectangle is in the range of 1.5 – 2.0. There is a faceted growing tendency on the surface of the polyhedral and a twin growing on the surface of the rectangular. The interface between Al_3Zr particulates and Al matrix is smooth, clean and there is no reaction product. Moreover, the observations in many samples show that the dislocation density of aluminum matrix nearby the polyhedral is higher than that of the matrix nearby the rectangular. The TEM diffraction pattern of the twinning is shown in Fig. 2(c). According to the diffraction pattern, it is determined that the twin plane is $(1\bar{1}\bar{4})$, the growth direction of the twin is $[\bar{2}21]$. The twinning growth model of Al_3Zr crystal is illustrated in Fig. 2(d).

What is the relation between the twin and the growing morphology of Al_3Zr intermetallics? Based on experimental observation and crystal growth theory[9], Al_3Zr intermetallic compound grows in the form of facet. The atomic arrangement on the interface of liquid/solid is smooth. Thus single molecule is difficult to accumulate up on the smooth surface of Al_3Zr crystal. However, the twin occurs because of the atomic dismatch. It results in a very pronounced reentrant edge or groove. The diffusing Al_3Zr molecules from the liquid melt are easy to attach to the groove. It may be concluded that the twin plane reentrant edge (TPRE)[10] is important here for the growth kinetics of Al_3Zr crystal. Although only one twin can be observed in Al_3Zr crystal, it is fact that there are four closely packed planes in Al_3Zr crystal, such as (114), $(\bar{1}\bar{1}4)$, $(1\bar{1}4)$ and $(\bar{1}14)$, according to the analysis of Al_3Zr crystal stereogram. The twinning phenomenon may take place on one or several

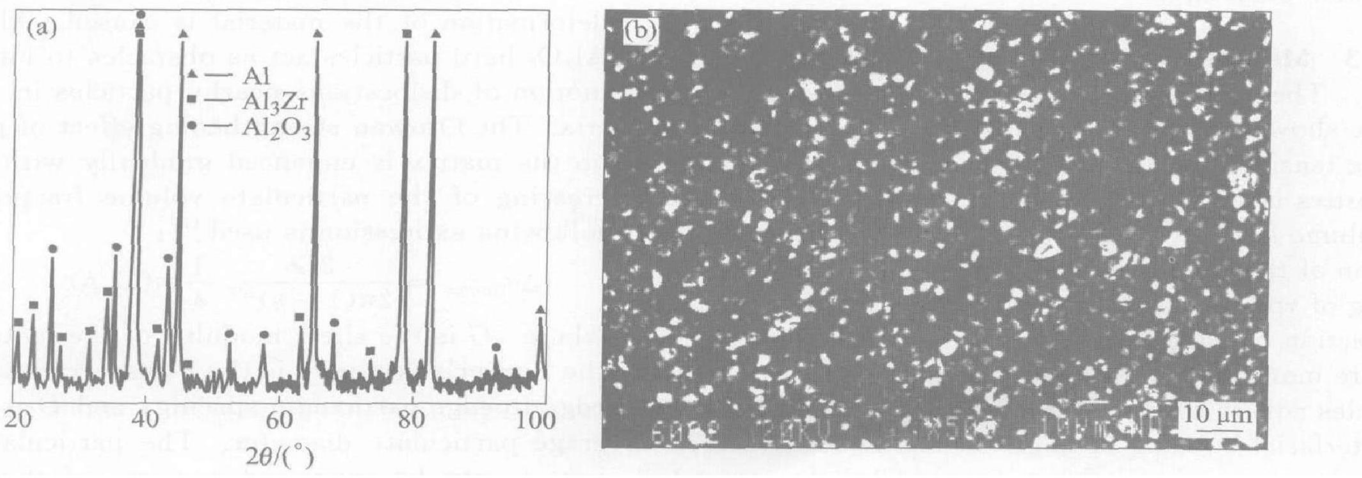

Fig. 1 XRD pattern(a) and SEM microstructure(b) of composite synthesized in Al-Zr-O system

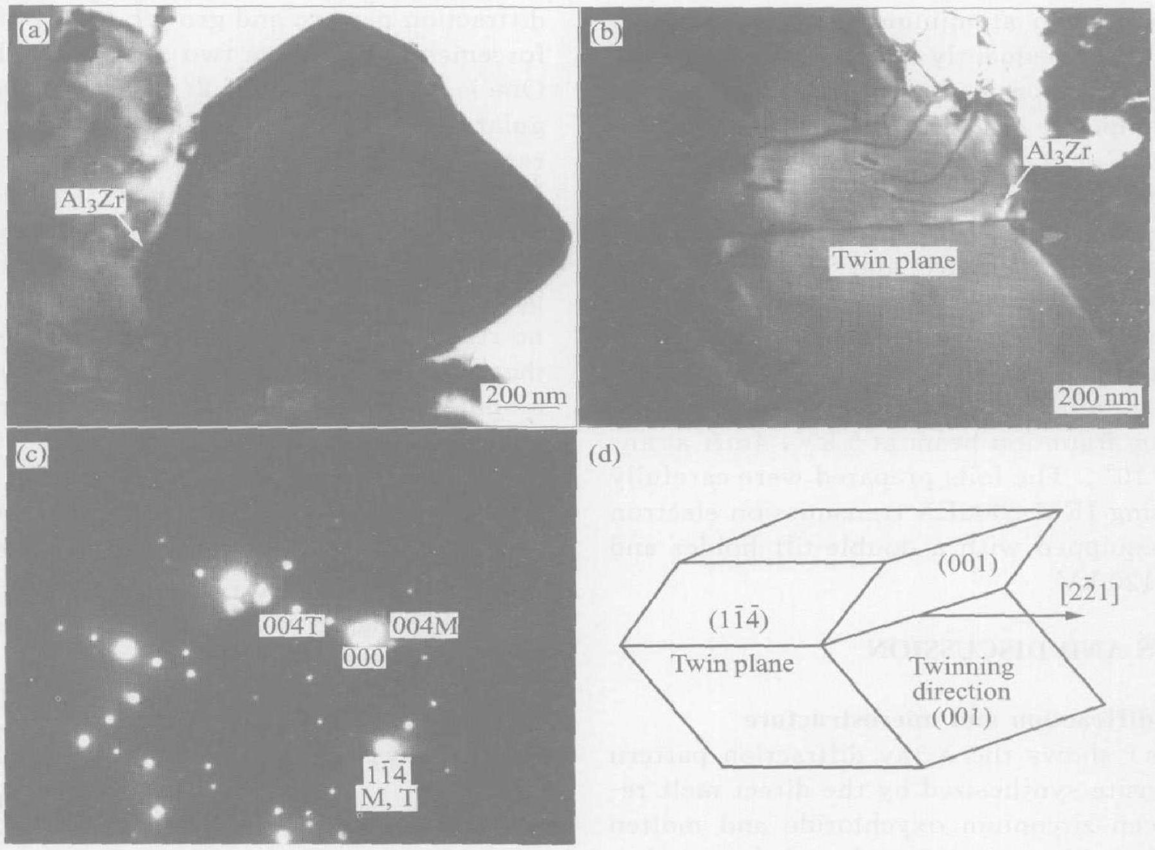

Fig. 2 Crystal morphologies and growth model of Al_3Zr
(a) —Polyhedral Al_3Zr crystal; (b) —Rectangular Al_3Zr crystal;
(c) —Diffraction pattern of twin; (d) —Growing model of Al_3Zr crystal

closely packed planes. So it can result in one twin or several twins. Under the observation of Al_3Zr morphology by SEM and TEM, Al_3Zr reinforcement grows in the shape of rectangle when only one twin is caused, whereas Al_3Zr reinforcement grows in the form of polyhedron when multiple twins are produced.

Fig. 3 shows the crystal morphology and TEM diffraction pattern of Al_2O_3 particle. It shows that the crystal morphology of Al_2O_3 particulate is approximately equiaxial, and Al_2O_3 crystal is of hexagonal structure.

3.3 Mechanical properties of composite

The mechanical properties of the composite are shown in Fig. 4(a). The result indicates that the tensile strength of $(Al_3Zr+Al_2O_3)_p/Al$ composites is enhanced greatly with the increasing of volume fraction of particles. However, the elongation of the composite is decreased with the increasing of volume fraction of particles when the volume fraction of particles is larger than 4%. The fracture morphology is shown in Fig. 4(b). Many particles adhere to the matrix. It is indicated that the interfacial bonding strength is high. The fracture of this composite is the mixture of brittleness and toughness. The principal strengthening mechanisms for $(Al_3Zr+Al_2O_3)_p/Al$ composites may include Orowan strengthening, grain-refined strengthening, solid-solution strengthening and dislocation strengthening. Linear summation of such terms may be used to predict yield strength and the results are

$$\sigma_{composite} = \Delta\sigma_{Orowan} + \Delta\sigma_{grain} + \Delta\sigma_{solution} + \Delta\sigma_{dislocation} \tag{5}$$

3.3.1 Orowan strengthening

Orowan strengthening results from interaction between the dislocation and the dispersed particles. When the composite bears the load the plastic deformation of the material is caused. Al_3Zr and Al_2O_3 hard particles act as obstacles to hinder the motion of dislocations nearby particles in the matrix. The Orowan strengthening effect of particles on the matrix is enhanced gradually with the increasing of the particulate volume fraction. The following expression is used[11]:

$$\Delta\sigma_{Orowan} = \frac{2Gb}{2\pi(1-\nu)^{1/2}}\frac{1}{\lambda}\ln(D/b) \tag{6}$$

where G is the shear modulus of the matrix, b is the Burger's vector, ν is the Poisson ratio, λ is the edge-to-edge particulate spacing, and D is the average particulate diameter. The particulate spacing, λ, can be expressed in terms of the volume fraction (φ) of dispersed particles and the average particulate diameter by[11]

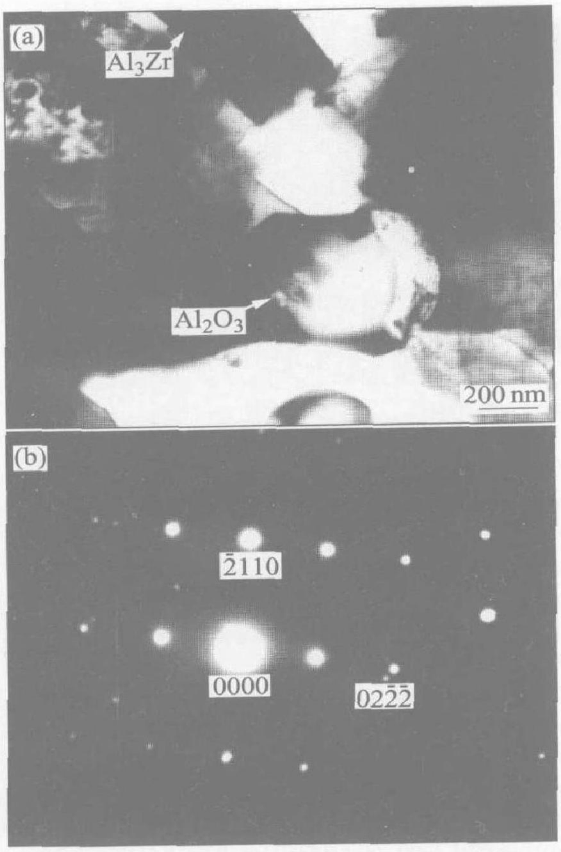

Fig. 3 TEM micrographs of in-situ Al_2O_3 particulate
(a) —Equiaxial Al_2O_3 particulate;
(b) —Diffraction pattern of [011̄2]

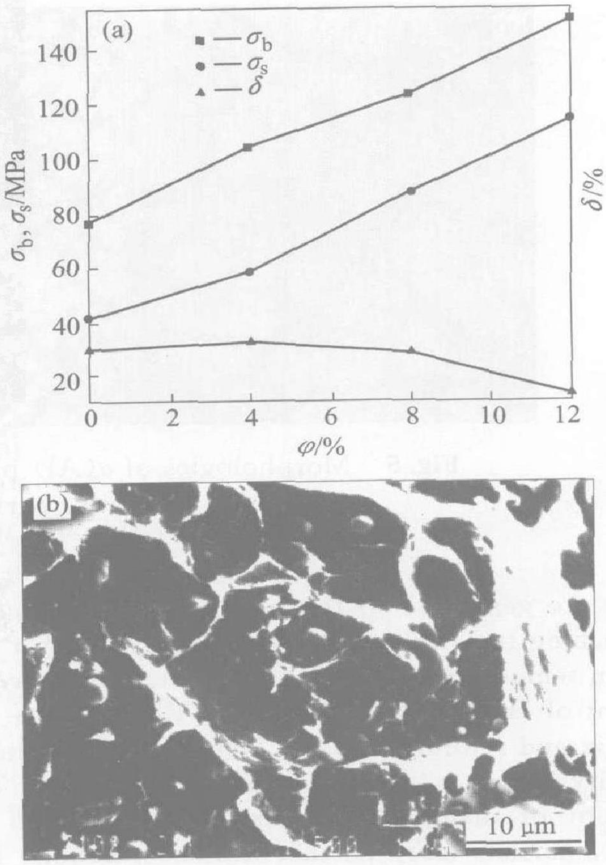

Fig. 4 Tensile property and fracture morphology of $(Al_3Zr+Al_2O_3)_p/Al$ composites at ambient temperature
(a) —Tensile property; (b) —Fracture morphology

$$\lambda = D\left[\frac{\pi}{6\varphi} - \frac{2}{3}\right]^{1/2} \tag{7}$$

which can be calculated with the microstructural parameters obtained from the TEM results. As concerned as for 12% $(Al_3Zr+Al_2O_3)_p/Al$ composite, where $G=26\,900$ MPa, $b=2.8\times10^{-10}$ m, $\nu=0.34$ and $D=0.5$ μm, the Orowan strengthening effect can be calculated by Eqns. (6) and (7) and the result is $\Delta\sigma_{Orowan}=23.01$ MPa.

3.3.2 Grain-refined strengthening

The experimental observations indicate that Al_3Zr reinforcing phase can reduce significantly the grain size of aluminum matrix with the increasing of the particulate volume fraction as shown in Fig. 5. According to the analysis of Al_3Zr crystal structure, polyhedral Al_3Zr particles act as the heterogeneous nucleation catalyst for aluminum. The grain-refined strengthening effect of Al_3Zr particulate is improved by the increasing of the volume fraction of polyhedral Al_3Zr particles via the Hall-Petch type of Eqn. (8)[12]:

$$\sigma_{grain} = \sigma_0 + kd^{-1/2} \tag{8}$$

where σ_{grain} is the yield strength contribution from grains, σ_0 is the friction stress, d is the grain size and k is the material constant. Thus, the grain-reinforced strengthening effect of 12% $(Al_3Zr+Al_2O_3)_p/Al$ composite can be obtained from Eqn. (9) and the value is $\Delta\sigma_{grain}=22.13$ MPa.

$$\Delta\sigma_{grain} = k(d_1^{-1/2} - d_2^{-1/2}) \approx kd_1^{-1/2} \tag{9}$$

where $k=0.07$ MPa·$m^{1/2}$ and $d_1=10$ μm.

3.3.3 Solid-solution strengthening

When a foreign zirconium (Zr) atom dissolves in the matrix aluminum (Al), it may act as an atomic-sized obstacle to the motion of dislocations. Because the volume of foreign Zr atom (0.023 272 nm^3) is larger than that of Al atom (0.016 603 nm^3), a misfit strain field will be produced around the Zr atom that may interact with the dislocation strain field. The analysis of the strain field-dislocation interaction is given by[13]

$$\Delta\sigma_{solution} = G\varepsilon\sqrt{x_f/4} \tag{10}$$

where G is the elastic shear modulus, x_f is the mole fraction of the foreign atoms and ε is the fractional difference in zirconium and aluminum atom diameters. So the solid-solution strengthening effect of 12% $(Al_3Zr+Al_2O_3)_p/Al$ composite can be evaluated by Eqn. (10) and the result is $\Delta\sigma_{solution}=35.79$ MPa. Where $G=26\,900$ MPa, $\varepsilon=0.119$, $x_f=0.05\%$.

3.3.4 Dislocation strengthening

In many of metal matrix composites, dislocations are generated in the matrix upon cooling or quenching temperature from the processing or so-

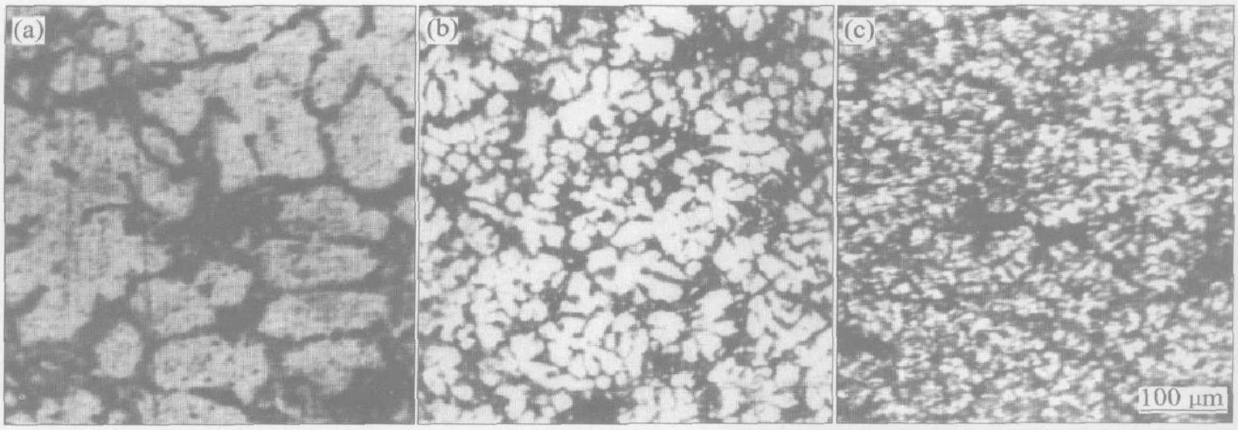

Fig. 5 Morphologies of α(Al) phase in $(Al_3Zr+Al_2O_3)_p/Al$ composite with different particulate volume fractions
(a) —φ= 0; (b) —φ= 8%; (c) —φ= 12%

lution temperature, due to a mismatch of the coefficient of thermal expansion (CTE) between the matrix and reinforcements. The higher dislocation density increases the strength of the matrix. The amount of dislocation generation is affected by CTE, particle size, particle volume fraction, and matrix strength. The dislocation strengthening effect of 12% $(Al_3Zr+Al_2O_3)_p/Al$ composite can be evaluated by[14]

$$\Delta\sigma_{dislocation} = AGb\sqrt{\Delta\rho} \qquad (11)$$

where A is the total surface areas of particles, G is the shear modulus of the matrix, b is the Burger's vector, and $\Delta\rho$ is the increment of dislocation density in the matrix because of particles. Thus, the dislocation strengthening result of 12% $(Al_3Zr+Al_2O_3)_p/Al$ composite is $\Delta\sigma_{dislocation}$ = 32.07 MPa. Where A = 0.83, G = 26 900 MPa, b = 2.8×10^{-10} m, $\Delta\rho = 2.52\times10^{13}$ m^{-2}.

According to Eqn.(5), the total yield strength of 12% $(Al_3Zr+Al_2O_3)_p/Al$ composite is calculated by $\sigma_{composite} = \Delta\sigma_{Orowan} + \Delta\sigma_{grain} + \Delta\sigma_{solution} + \Delta_{dislocation}$ = 113.0 MPa, whereas the real yield strength of this composite is measured to be 112.4 MPa by the tensile test. So the difference in yield strength of 12% $(Al_3Zr+Al_2O_3)_p/Al$ composite between the elevated value and the tested value is very approximate.

REFERENCES

[1] Nardone V C, Prewo K W. On the strength of discontinuous silicon carbide reinforced aluminum composites [J]. Scripta Metall, 1986, 20(1): 43 - 48.

[2] Ibrahim L A, Mohamed F A, Lavernia E J. Particulate reinforced metal matrix composites —A review[J]. J Mater Sci, 1991, 26: 1137 - 1156.

[3] Rohatgi P K. Future directions in solidification of metal matrix composites[J]. Key Eng Mater, 1995, 104: 293 - 297.

[4] Zhao Y T, Sun G X. In situ synthesis of novel composites in the system Al-Zr-O[J]. J Mater Sci Lett, 2001, 20 (20): 1859 - 1861.

[5] Mitra R, Fine E M, Weertman J R. Chemical reaction strengthening of Al/TiC metal matrix composites by isothermal heat treatment at 913 K[J]. J Mater Res, 1993, 8(9): 2370 - 2376.

[6] Nakata H, Choh T, Kanetake N. Fabrication and mechanical properties of in situ formed carbide particulate reinforced aluminum composite[J]. J Mater Sci, 1995, 30: 1719 - 1729.

[7] Tong X C, Fang H S. Al-TiC composites in situ-processed by ingot metallurgy and rapid solidification technology: part II. Mechanical behavior[J]. Metall Mater Trans A, 1998, 29A: 893 - 902.

[8] Wood J V, Davies P, Kellie J L F. Properties of reactively cast aluminum-TiB_2 alloys[J]. Mater Sci Tech, 1993, 9: 833 - 840.

[9] ZHAO Yu-tao, SUN Guo-xiong. Twin growth of in-situ formed Al_3Zr in the system Al-$ZrOCl_2$[J]. Chinese Journal of Materials Research, 2001, 15 (4): 420 - 424. (in Chinese)

[10] Hashimoto S, Yamaguchi A, Yasuda M. Fabrication and properties of novel composites in the system Al-Zr-C [J]. J Mater Sci, 1998, 33: 4835 - 4842.

[11] Tong X C, Ghosh A K. Fabrication of in situ TiC reinforced aluminum matrix composites [J]. J Mater Sci, 2001, 36(16): 4059 - 4069.

[12] Lloyd D J. Particle reinforced aluminum and magnesium matrix composites [J]. International Materials Reviews, 1994, 39(1): 1 - 23.

[13] Verhoeven J D. Fundamentals of Physical Metallurgy [M]. New York: John Wiley & Sons Inc, 1975. 518 - 524.

[14] Clyne T W, Withers P J. Euromat 91: Proceedings of the 2nd European Conference on Advanced Materials and Processes[M]. University of Combridge: Institute of Metals, 1991. 56 - 64.

(Edited by YUAN Sai-qian)